

STM/STS study of the superconducting gap in $\text{SmFeAsO}_{1-x}\text{F}_x$ 

Yuki Kawashima^{a,*}, Koichi Ichimura^{a,b}, Kazuhiro Katono^a, Tohru Kurosawa^{b,c},
Migaku Oda^{b,c}, Satoshi Tanda^{a,b}, Yoichi Kamihara^d, Hideo Hosono^e

^a Department of Applied Physics, Hokkaido University, Sapporo 060-8628, Japan

^b Center of Education and Research for Topological Science and Technology, Hokkaido University, Sapporo 060-8628, Japan

^c Department of Physics, Hokkaido University, Sapporo 060-0810, Japan

^d Department of Applied Physics and Physico-Informatics, Keio University, Yokohama 223-8522, Japan

^e Frontier Research Center, Tokyo Institute of Technology – Yokohama 226-8503, Japan

ARTICLE INFO

Article history:

Received 17 October 2014

Received in revised form

26 November 2014

Accepted 4 December 2014

Communicated by H. Akai

Available online 11 December 2014

Keywords:

A. Iron-based superconductor

D. Superconducting gap

E. STM

ABSTRACT

We report an electron tunneling study of $\text{SmFeAsO}_{1-x}\text{F}_x$ in the low doping region ($x=0, 0.045, 0.046, 0.069$) by low temperature UHV-STM/STS. Superconducting gaps are observed for each superconducting sample $x=0.045$ ($T_c=12.9$ K), $x=0.046$ ($T_c=32.9$ K) and $x=0.069$ ($T_c=46.9$ K). We obtained corresponding superconducting gap size of $\Delta_{\text{SC}}=9.5 \pm 0.5$ meV, 9.75 ± 0.25 meV and 11 ± 1 meV. While T_c increases, Δ_{SC} is kept the same. This suggests that the effective attractive interaction is the same and that there is some mechanism that suppresses the superconductivity in the low doping region. On the other hand, similar gap structures were found in a non-superconducting sample with $x=0$ at 7.8 K. The obtained gap size was $\Delta_{\text{N}}=8.5 \pm 1.5$ meV, which is almost the same as the superconducting gap in the superconducting samples ($x=0.045, 0.046, 0.069$).

© 2014 Published by Elsevier Ltd.

1. Introduction

Iron-based superconductors were discovered as a new class of high critical temperature T_c superconductor with a two-dimensional structure [1,2]. These superconductors have a high critical temperature and offer the possibility of a new superconducting mechanism thus making them a high impact material. Iron-based superconductors have different types of crystal structures including RFePnO (R=rare earth metals, Pn=P, As) [1,2], BaFe_2As_2 [3], LiFeAs [4] and FeSe_{1- δ} [5]. The RFePnO group has the highest T_c among iron-based superconductors. The phase diagram has been studied over a wide range of doping levels by employing hydrogen substitution on LaFeAsO [6]. Iron-based superconductors generally have the magnetic phase next to the superconducting phase. One can imagine that the superconductivity has a magnetic origin in iron-based superconductors. The itinerant antiferromagnetic ordered phase is stable for the mother compound of iron-based superconductors [7,8], unlike high- T_c cuprates, whose magnetic phase is a Mott insulator. It is important to study the magnetic phase to clarify the origin of the superconductivity in iron-based superconductors. With RFePnO, the ground state is controlled by the carrier concentration. $\text{SmFeAsO}_{1-x}\text{F}_x$ has the highest T_c of RFeAsO_{1-x}F_x system materials [9,10]. The T_c of $\text{SmFeAsO}_{1-x}\text{F}_x$ increases to 58.1 K and is very sensitive to

fluorine substitution [11,12]. Therefore, investigating the superconductivity of $\text{SmFeAsO}_{1-x}\text{F}_x$ is a valuable method for understanding iron-based superconductors. $\text{SmFeAsO}_{1-x}\text{F}_x$ is useful when discussing the difference between the electronic states of the magnetic and superconducting phases because its higher T_c increase the superconducting order parameter. The doping dependence of the crystal structure on $\text{SmFeAsO}_{1-x}\text{F}_x$ was studied by using high resolution X-ray diffraction at several fluorine concentrations [13]. Spectroscopic studies have been needed to investigate the superconductivity with the systematic substitution of fluorine in $\text{SmFeAsO}_{1-x}\text{F}_x$.

Electron tunneling is useful for revealing the mechanism of the superconductivity [14]. It is a direct method for obtaining the energy spectrum of the electronic density of states. Because scanning tunneling microscopy/spectroscopy (STM/STS) observes the electronic state in a local area within a few atoms, STM can probe a single crystalline domain in a polycrystalline sample. Using STM, we can obtain the energy spectra of the density of states with high energy resolution by measuring the tunneling differential conductance, and the electron density with a nano-scale spatial resolution. Therefore, we can obtain the spatial variation of the superconducting gap with atomic resolution. The gap anisotropy can be studied directly with the STM/STS technique by probing the local density of states at various crystal surfaces [15]. Since the tip of the probe does not come in contact with the sample, STM/STS is a nondestructive method. Various STM studies have been undertaken on the surface structure and the gap symmetry in iron-based superconductors [16]. Recently, an STM study revealed a charge stripe structure on FeTe [17].

* Corresponding author. Tel.: +81 11 706 7818

E-mail address: yuki-k@eng.hokudai.ac.jp (Y. Kawashima).

STM/STS [18] and photoemission spectroscopy [19,20] have been used to observe the superconducting gap and pseudogap of LaFeAsO_{1-x}F_x. The superconducting gap of F-doped SmFeAsO was observed by point contact measurement [21] and of SmFeAsO_{1-δ} by STM [22]. Tunneling spectroscopy is needed for SmFeAsO_{1-x}F_x in the lower fluorine concentration region, where the boundary between the superconducting and non-superconducting phases is located. We study the electronic state of SmFeAsO_{1-x}F_x with several fluorine concentrations by using STM/STS and discuss the superconducting gap depending on T_c .

2. Experimental

The procedure for synthesizing polycrystalline SmFeAsO_{1-x}F_x ($x=0.045, 0.046, 0.069$) is reported in reference [11]. The F content (x) of samples was obtained according to Vegard's volume rule [23]. The superconducting transition temperatures for $x=0.045, 0.046$ and 0.069 were determined as 12.9 K, 32.9 K and 46.9 K, respectively, from resistivity measurements. An undoped SmFeAsO sample does not exhibit superconductivity in a resistivity measurement. Temperature variable ultra high vacuum (UHV)-STM was used in the STM/STS study. Pr-Ir alloy wire was used as the scanning tip. Block shaped samples were cracked just before being transferred into the UHV-STM chamber to obtain a fresh surface. The tunneling differential conductance at 7 K and 80 K was directly measured with the standard lock-in technique with a 5 kHz ac modulation of 3 mV added to the bias voltage.

3. Results and discussion

Fig. 1(a) and (b) shows a typical normalized tunneling conductance dI/dV curve for SmFeAsO_{1-x}F_x ($x=0.069, T_c=46.9$ K) at 7.3 K and its numerical differential d^2I/dV^2 , respectively. The conductance curves have a slight spatial dependence. They are almost identical

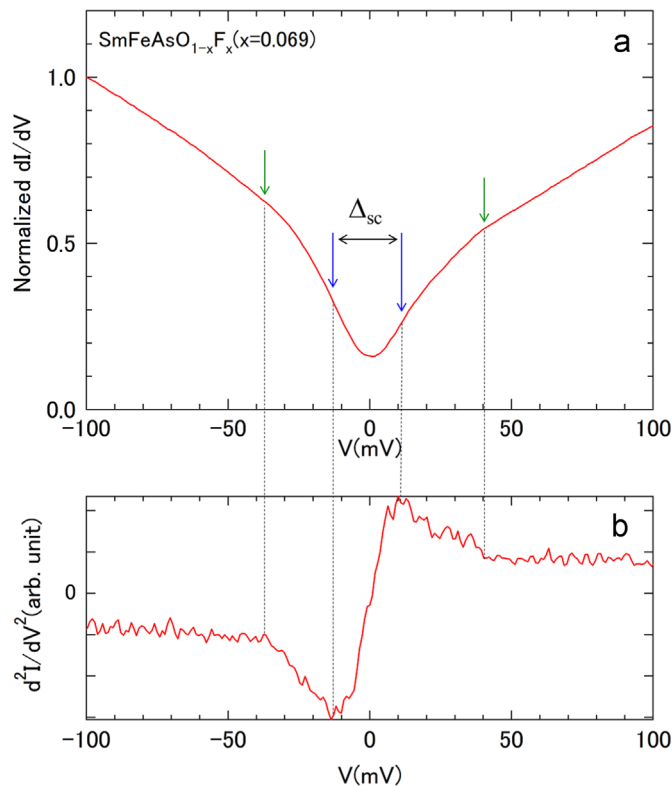


Fig. 1. (Color online) (a) Tunnel differential conductance of SmFeAsO_{1-x}F_x ($x=0.069, T_c=46.9$ K) at 7.3 K. (b) Numerical differential of the conductance curve shown in (a).

regardless of the distance between the tip and the sample at the same position. As shown in Fig. 1(a), the tunneling differential conductance is reduced around the zero bias voltage, and this is associated with the superconducting state. The conductance peaks at gap edges do not appear in the tunneling spectra. There is a kink structure around $|V|=12$ mV indicated by blue arrows, which corresponds to the peak and dip in the d^2I/dV^2 curve. We confirmed that the differential conductance curve at 80 K is featureless. It means that the kink structures around $|V|=12$ mV do not exist at 80 K. We define the kink structures indicated by the blue arrows as the superconducting gap. We also found the pseudogap structure in the form of other kinks around $|V|=36$ mV and shown by green arrows. These structures were determined in the same manner as with LaFeAsO_{1-x}F_x [18]. We obtained the superconducting gap $\Delta_{sc}=12$ meV and the pseudogap $\Delta_{PG}=36$ meV for these data. For several data, we obtained $\Delta_{sc}=11 \pm 1$ meV for SmFeAsO_{1-x}F_x ($x=0.069$), correspondingly $2\Delta_{sc}/kT_c=5.41 \pm 0.52$. The pseudogap was obtained as $\Delta_{PG}=25-42.5$ meV.

Fig. 2(a) and (b) shows typical normalized tunneling conductance dI/dV curves for $x=0.046$ ($T_c=32.9$ K) at 7.5 K and $x=0.045$ ($T_c=12.9$ K) at 7.8 K, respectively. Tunneling spectra for $x=0.045$ and $x=0.046$ samples have similar structures to that for the $x=0.069$ sample. We define the superconducting gap and pseudogap in the same manner as described above. The kink structures corresponding to the superconducting gap can be seen around $|V|=9.5$ mV in Fig. 2 (a) and (b) and are indicated by blue arrows. We obtained Δ_{sc} as 9.75 ± 0.25 meV and 9.5 ± 0.5 meV for $x=0.046$ and $x=0.045$,

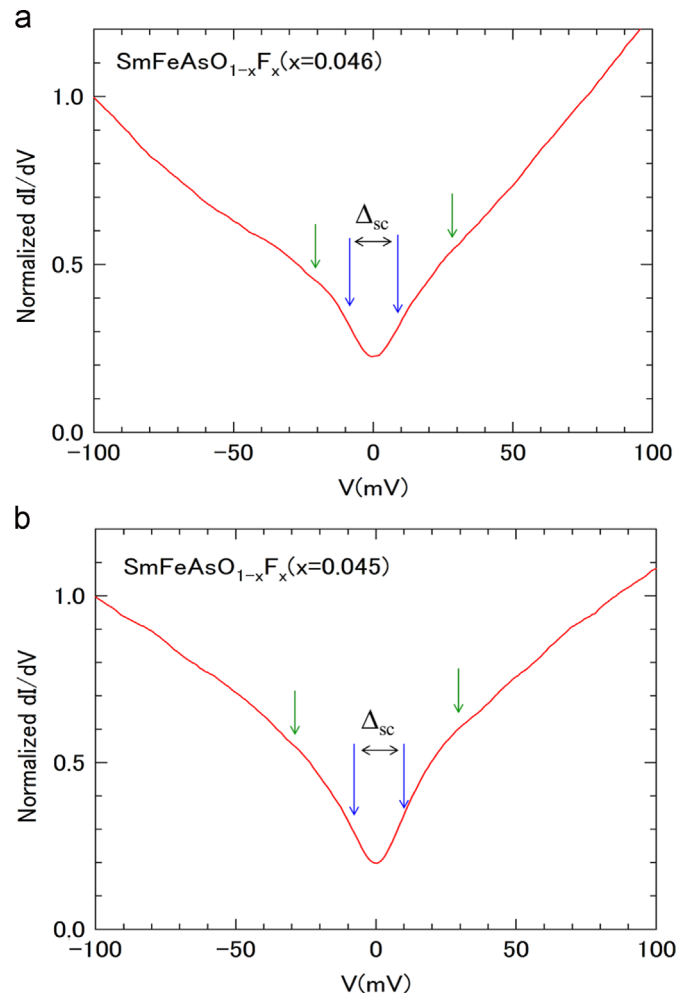


Fig. 2. (Color online) (a) and (b) show tunnel differential conductances for $x=0.046$ ($T_c=32.9$ K) at 7.5 K and $x=0.045$ ($T_c=12.9$ K) at 7.8 K, respectively.

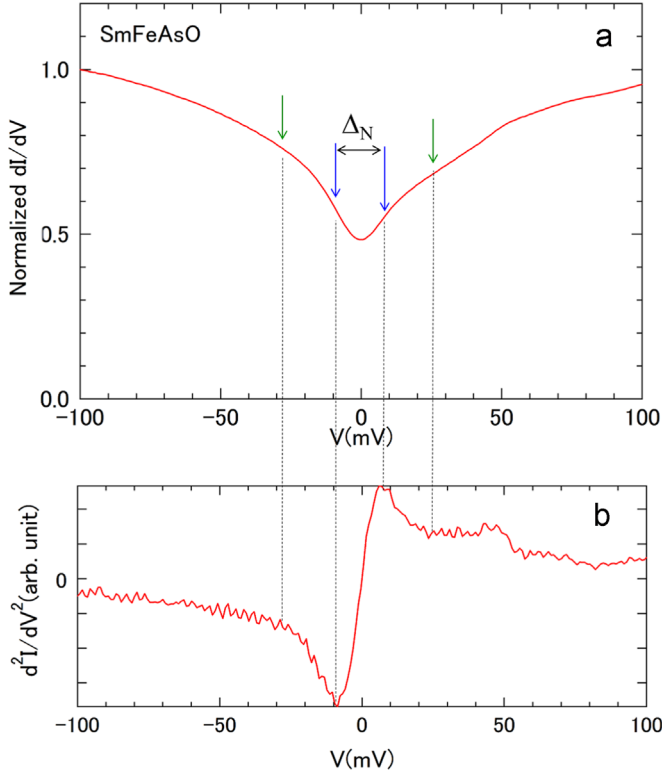


Fig. 3. (Color online) (a) Tunnel differential conductance of undoped SmFeAsO at 7.8 K. (b) Numerical differential of the conductance curve shown in (a).

respectively. The corresponding $2\Delta_{SC}/kT_c$ values were estimated to be 6.87 ± 0.18 and 17.08 ± 0.9 for $x=0.046$ and $x=0.045$, respectively. Pseudogaps of $\Delta_{PG} = 22.5\text{--}94$ meV and $25\text{--}70$ meV were obtained for $x=0.046$ and $x=0.045$, respectively.

Fig. 3(a) and (b) shows a typical normalized tunneling conductance dI/dV curve for undoped SmFeAsO and its numerical differential d^2I/dV^2 at 7.8 K, respectively. The conductance at $V=0$ is larger than that of superconducting samples ($x=0.045, 0.046, 0.069$), suggesting greater lifetime broadening [24]. It is noteworthy that the anomalies indicated by the blue arrows are similar to the superconducting gap structure observed in the superconducting samples. However, undoped SmFeAsO does not exhibit superconductivity in the bulk resistivity measurement. Then we define the gap Δ_N of undoped SmFeAsO. The pseudogap indicated by the green arrows was also found. We obtained $\Delta_N = 8.5 \pm 1.5$ meV and pseudogap $\Delta_{PG} = 16\text{--}48$ meV for undoped SmFeAsO.

Our obtained $T_c, \Delta_{SC}(\Delta_N), 2\Delta_{SC}/kT_c$ and Δ_{PG} values are listed in Table 1. Fig. 4 shows Δ_{SC}, Δ_N and T_c as a function of x . When we compare results for $x=0.045$ and $x=0.046$, the T_c changes rapidly from 12.9 K to 32.9 K, while the superconducting gap remains almost the same. The T_c increases linearly at $x \geq 0.046$. Δ_{SC} for $x=0.069$ is larger than that for $x=0.046$. However, there is only a slight change in the superconducting gap. The $2\Delta_{SC}/kT_c$ values for SmFeAsO $_{1-x}$ F $_x$ are $17.08 \pm 0.9, 6.87 \pm 0.18$ and 5.41 ± 0.52 for $x=0.045, 0.046$ and 0.069 , respectively. Our results show that $2\Delta_{SC}/kT_c$ decreases with increasing x and is larger than the BCS value of 3.52 for $x=0.045, 0.046$ and 0.069 . On the other hand, the $2\Delta_{SC}/kT_c$ value at a higher doping level is reported to be 3.68 for F-doped SmFeAsO [21] and 3.55–3.8 for SmFeAsO $_{1-\delta}$ [22]. These values are fairly consistent with the BCS value. We deduce that $2\Delta_{SC}/kT_c$ merges with the BCS value as the carrier concentration increases. Our results show that both Δ_{SC} and T_c increase with increasing x . However, the variation in Δ_{SC} is smaller than that of T_c . As a consequence, $2\Delta_{SC}/kT_c$ decreases as T_c increases. We emphasize that the variation in Δ_{SC} is very small. Δ_{SC} generally corresponds

Table 1

$T_c, \Delta_{SC}, 2\Delta_{SC}/kT_c$ and Δ_{PG} for $x=0, 0.045, 0.046$ and 0.069 .

x	0	0.045	0.046	0.069
T_c (K)	—	12.9	32.9	46.9
Δ_{SC} (meV)	($\Delta_N = 8.5 \pm 1.5$)	9.5 ± 0.5	9.75 ± 0.25	11 ± 1
$2\Delta_{SC}/kT_c$	—	17.08 ± 0.9	6.87 ± 0.18	5.41 ± 0.52
Δ_{PG} (meV)	16–48	25–70	22.5–94	25–42.5

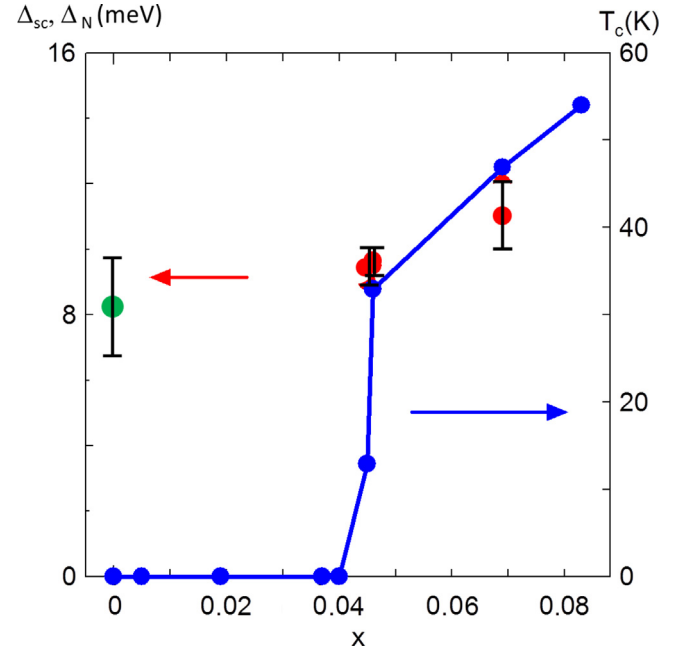


Fig. 4. (Color online) Δ_{SC}, Δ_N and T_c as a function of x . Red, green and blue dots show Δ_{SC}, Δ_N and T_c , respectively.

to the strength of the attractive interaction. We suggest that the attractive interaction is slightly changed by the substitution level, although T_c varies significantly. In other words, there is some mechanism that suppresses the superconductivity while the interaction remains almost constant.

A superconducting gap like structure Δ_N exists on undoped SmFeAsO, where no superconducting transition was observed in the resistivity measurement. There is a possibility that Δ_N is associated with the antiferromagnetic order [11,25,26]. From the observed $\Delta_N = 8.5$ meV, the antiferromagnetic transition temperature T_N is expected to be 55.7 K based on the mean field theory. However, the observed $T_N = 144$ K [11] is far higher than the value expected from Δ_N . Then it is difficult to relate Δ_N to the antiferromagnetic order. The energy scale of Δ_N can be reasonably associated with the maximum superconducting transition temperature on SmFeAsO $_{1-x}$ F $_x$ ($T_c = 58.1$ K). This should be noted that the gap $\Delta_N = 8.5 \pm 1.5$ meV found for $x=0$ has the same energy scale as the superconducting gap for $x=0.045, 0.046$ and 0.069 . This suggests that the attractive potential exists even in the non-superconducting phase with the same strength as that in the superconducting phase. The substitution of fluorine leads to the bulk superconductivity of SmFeAsO $_{1-x}$ F $_x$.

The pseudogap structure was observed for all SmFeAsO $_{1-x}$ F $_x$ ($x=0, 0.045, 0.046, 0.069$) as listed in Table 1, which is similar to the result for LaFeAsO $_{1-x}$ F $_x$ [18]. For some reason the obtained values are scattered. However, the magnitude of the pseudogap is tens of meV for all x in the present study. This is largely consistent with the value $\Delta_{PG} = 60$ meV for F-doped SmFeAsO $_{1-\delta}$ obtained with time-domain spectroscopy [27]. The pseudogap is thought to be a common feature in iron-based superconductors. The relationship

between the pseudogap and the superconductivity remains still an open problem.

4. Summary

We undertook a systematic study of the electronic state of $\text{SmFeAsO}_{1-x}\text{F}_x$ at a low doping level. The superconducting gap and the pseudogap structure were observed for superconducting samples ($x=0.045, 0.046, 0.069$). We found the size of the superconducting gap to be almost the same irrespective of the fluorine concentration, while T_c increased as the doping level increased. The result suggests that the attractive interaction is constant irrespective of the doping level and a mechanism that suppresses T_c . Fluorine substitution weakens the suppression of the superconducting transition. In a non-superconducting sample ($x=0$), we found the gap structure Δ_N , which is similar to the gap Δ_{SC} in the superconducting samples. The energy scale of Δ_N can be reasonably associated with the maximum superconducting transition temperature of $\text{SmFeAsO}_{1-x}\text{F}_x$ ($T_c=58.1$ K). The finding suggests that an attractive interaction potentially exists even in the non-superconducting phase.

Acknowledgments

This work was supported by the 21COE program on “Topological Science and Technology” of the Ministry of Education, Culture, Sport, Science and Technology of Japan. This work was partially supported by the Asahi Glass Foundation, and the Japan Society for Promotion of Science (JSPS) KAKENHI Grant no. 26400337.

References

- [1] Y. Kamihara, H. Hiramatsu, M. Hirano, R. Kawamura, H. Yanagi, T. Kamiyama, H. Hosono, *J. Am. Chem. Soc.* 128 (2006) 10012.
- [2] Y. Kamihara, T. Watanabe, M. Hirano, H. Hosono, *J. Am. Chem. Soc.* 130 (2008) 107006.
- [3] M. Rotter, M. Tegel, D. Johrendt, *Phys. Rev. Lett.* 101 (2008) 9691.
- [4] J.H. Tapp, Z. Tang, B. Lv, K. Sasmal, B. Lorenz, P.C.W. Chu, A.M. Guloy, *Phys. Rev. B* 78 (2008) 060505.
- [5] F.-C. Hsu, J.-Y. Luo, K.-W. Yeh, T.-K. Chen, T.-W. Huang, P.M. Wu, Y.-C. Lee, Y.-L. Huang, Y.-Y. Chu, D.-C. Yan, M.-K. Wu, *Proc. Natl. Acad. Sci. USA* 105 (2011) 14262.
- [6] S. Iimura, S. Matsuishi, H. Sato, T. Hanna, Y. Muraba, S.W. Kim, J. Eun Kim, M. Takata, H. Hosono, *Nat. Commun.* 3 (2013) 943.
- [7] C. de la Cruz, Q. Huang, J.W. Lynn, J. Li, W.R.I. An, J.L. Zarestky, H.A. Mook, G.F. Chen, J.L. Luo, N.L. Wang, P. Dai, *Nature* 453 (2008) 899.
- [8] Q. Huang, Y. Qiu, W. Bao, M.A. Green, J.W. Lynn, Y.C. Gasparovic, T. Wu, G. Wu, X.H. Chen, *Phys. Rev. Lett.* 101 (2008) 257003.
- [9] Y. Chen, Y. Cui, C. Cheng, Y. Yang, L. Wang, Y. Li, Y. Zhang, Y. Zhao, *Phys. C: Superconduct.* 470 (2010) 989.
- [10] X.H. Chen, T. Wu, G. Wu, R.H. Liu, H. Chen, D.F. Fang, *Nature* 453 (2008) 761.
- [11] Y. Kamihara, T. Nomura, M. Hirano, J.E. Kim, K. Kato, M. Takata, Y. Kobayashi, S. Kitao, S. Higashitaniguchi, Y. Yoda, M. Seto, H. Hosono, *New J. Phys.* 12 (2010) 033005.
- [12] M. Fujioka, S.J. Denholme, T. Ozaki, H. Okazaki, K. Deguchi, S. Demura, H. Hara, T. Watanabe, H. Takeya, T. Yamaguchi, H. Kumakura, Y. Takano, *Superconduct. Sci. Tech.* 26 (2013) 085023.
- [13] S. Margadonna, Y. Takabayashi, M.T. McDonald, M. Brunelli, G. Wu, R.H. Liu, X.H. Chen, K. Prassides, *Phys. Rev. B* 79 (2009) 014503.
- [14] I. Giaever, K. Megerle, *Phys. Rev.* 122 (1961) 1101.
- [15] K. Ichimura, K. Nomura, *J. Phys. Soc. Jpn.* 75 (2006) 051012.
- [16] J.E. Hoffman, *Rep. Prog. Phys.* 74 (2011) 124513.
- [17] Y. Kawashima, K. Ichimura, J. Ishioka, T. Kurosawa, M. Oda, K. Yamaya, S. Tanda, *Solid State Commun.* 167 (2013) 10.
- [18] K. Ichimura, J. Ishioka, T. Kurosawa, K. Inagaki, M. Oda, S. Tanda, H. Takahashi, H. Okada, Y. Kamihara, M. Hirano, H. Hosono, *J. Phys. Soc. Jpn.* 77 (Suppl.) (2008) 151.
- [19] T. Sato, S. Souma, K. Nakayama, K. Terashima, K. Sugawara, T. Takahashi, Y. Kamihara, M. Hirano, H. Hosono, *J. Phys. Soc. Jpn.* 77 (2008) 063708.
- [20] Y. Ishida, T. Shimojima, K. Ishizaka, T. Kiss, M. Okawa, T. Togashi, S. Watanabe, X. Wang, C. Chen, Y. Kamihara, M. Hirano, H. Hosono, S. Shin, *Phys. Rev. B* 79 (2009) 060503.
- [21] T.Y. Chen, Z. Tesanovic, R.H. Liu, X.H. Chen, C.L. Chien, *Nature* 453 (2008) 1224.
- [22] O. Millo, I. Asulin, O. Yuli, I. Felner, Z.A. Ren, X.L. Shen, G.C. Che, Z.X. Zhao, *Phys. Rev. B* 78 (2008) 092505.
- [23] A. Cox, M.J.L. Sangster, *J. Phys. C: Solid State Phys.* 18 (1985) L1123.
- [24] R.C. Dynes, V. Narayanamurti, J.P. Garno, *Phys. Rev. Lett.* 41 (1978) 1509.
- [25] M. Tropeano, A. Martinelli, A. Palenzona, E. Bellingeri, E. Galleani d’Agliano, T.D. Nguyen, M. Affronte, M. Putti, *Phys. Rev. B* 78 (2008) 094518.
- [26] R.H. Liu, G. Wu, T. Wu, D.F. Fang, H. Chen, S.Y. Li, K. Liu, Y.L. Xie, X.F. Wang, R.L. Yang, L. Ding, C. He, D.L. Feng, X.H. Chen, *Phys. Rev. Lett.* 101 (2008) 087001.
- [27] T. Mertelj, P. Kusar, V.V. Kabanov, L. Stojchevska, N.D. Zhigadlo, S. Katrych, Z. Bukowski, J. Karpinski, S. Weyeneth, D. Mihailovic, *Phys. Rev. B* 81 (2010) 224504.